Interaction of Collagen-Like Peptide Models of Asymmetric Acetylcholinesterase with Glycosaminoglycans: Spectroscopic Studies of Conformational Changes and Stability†

Ellen Doss-Pepe,‡ Paola Deprez,‖ Nibaldo C. Inestrosa,‖ and Barbara Brodsky*,‡

Department of Biochemistry, UMDNJ-Robert Wood Johnson Medical School, Piscataway, New Jersey 08854 and the Centro de Regulación Celular y Patología, Departamento de Biología Celular y Molecular, Facultad de Ciencias Biológicas, Pontificia Universidad Católica de Chile, Santiago, Chile

Received May 16, 2000; Revised Manuscript Received October 3, 2000

ABSTRACT: The effect of heparin on the conformation and stability of triple-helical peptide models of the collagen tail of asymmetric acetylcholinesterase expands our understanding of heparin interactions with proteins and presents an opportunity for clarifying the nature of binding of ligands to collagen triple-helix domains. Within the collagen tail of AChE, there are two consensus sequences for heparin binding of the form BBXB, surrounded by additional basic residues. Circular dichroism studies were used to determine the effect of the addition of increasing concentrations of heparin on triple-helical peptide models for the heparin binding domains, including peptides in which the basic residues within and surrounding the consensus sequence were replaced by alanine residues. The addition of heparin caused an increased triple-helix content with saturation properties for the peptide modeling the C-terminal site, while precipitation, with no increased helix content resulted from heparin addition to the peptide modeling the N-terminal site. The results suggest that the two binding sites with a similar triple-helical conformation have distinctive ways of interacting with heparin, which must relate to small differences in the consensus sequence (GRKGR vs GKRGK) and in the surrounding basic residues. Addition of heparin increased the thermal stability of all peptides containing the consensus sequence. Heparan sulfate produced conformational and stabilization effects similar to those of heparin, while chondroitin sulfate led to a cloudy solution, loss of circular dichroism signal, and a smaller increase in thermal stability. Thus, specificity in both the sequence of the triple helix and the type of glycosaminoglycan is required for this interaction.

Asymmetric acetylcholinesterase (AChE, EC 3.1.1.7)[1] catalyzes the hydrolysis of acetylcholine and is involved in the termination of signal release from nerve endings, thereby regulating the transmission of neuromuscular signals and, ultimately, muscle contraction (*1*, *2*). The asymmetric form of AChE is concentrated at vertebrate neuromuscular junctions and contains a covalently attached collagen tail that is responsible for the anchorage and specific localization of the catalytic tetramers to the synaptic basal lamina (*3*−*7*). This integration is thought to be mediated by the interaction of the collagen tail with heparan sulfate proteoglycans (HSPGs) (*8*). Heparan sulfate (HS) is composed of repeating dissacharide units with heterogeneous sulfation and is attached to a protein core to form HSPG. Evidence for the interaction between the collagen tail and glycosaminoglycans (GAGs) of HSPGs was provided by experiments in which HS was able to solubilize asymmetric AChE from neuromuscular tissue (*8*, *9*). Heparin, which has a similar sugar composition but a higher degree of sulfation than heparan sulfate, was also able to release AChE, while chondroitin sulfate, which differs in disaccharide composition, did not (*8*, *9*). This makes heparin a useful model for studying HSPG−protein interactions. In this study, heparin was used as a model to examine the interaction of heparan sulfate proteoglycans with the collagen tail of AChE.

The central collagen-like region of the tail of asymmetric AChE contains two basic regions that are heparin-binding consensus sequences: residues 149−152 (GRKGR) and residues 254−257 (GKRGK) (*10*). These two sequences are of the form B−B−X−B (where B represents a basic residue), a pattern representing one of the heparin-binding consensus sequences described for globular proteins (*11*, *12*). Heparin binding sites have also been described in collagen types I, IV, and V, and these sequences contain clusters of basic residues that do not follow identified consensus patterns (*13*−*19*).

† This work was supported by the NIH grant GM60048 (to B.B.), the FONDECYT Grant No. 2970072 (to P.D.), and the FONDAP Grant No. 13980001 and a Presidential Chair in Science (1999−2001) from the Chilean Government (to N.C.I.).

* To whom correspondence should be addressed: Department of Biochemistry, UMDNJ-Robert Wood Johnson Medical School, Piscataway, NJ 08854

‡ UMDNJ-Robert Wood Johnson Medical School.

‖ Pontificia Universidad Católica de Chile.

[1] Abbreviations: AChE, acetylcholinesterase; HSPG, heparan sulfate proteoglycan; GAG, glycosaminoglycan; HS, heparan sulfate; CS, chondroitin sulfate; CD, circular dichroism spectroscopy; [θ], mean residue ellipticity; MW, molecular weight; T_m, melting temperature; standard single letter and three letter codes have been used to denote common amino acids; hydroxyproline is denoted by O (single letter code) and Hyp (three letter code).

10.1021/bi001108u CCC: $19.00
Published on Web 11/10/2000

The triple-helix conformation, as found in collagens, asymmetric AChE, and host defense proteins, consists of three supercoiled polyproline II-like chains that are staggered by one residue and stabilized by hydrogen bonding between three chains (*20*−*23*). To allow for the close packing of the triple helix, every third residue near the center of the supercoiled helix must be a glycine, generating a $(Gly-X-Y)_n$ repeating sequence pattern. The solvent-accessible X and Y positions are frequently occupied by Pro and Hyp residues, respectively (*24*), with Gly−Pro−Hyp being the most stable tripeptide unit for the triple-helix conformation (*25*−*27*). Within the collagen tail of AChE, the two heparin binding consensus sequences, GRKGR and GKRGK, are both part of the Gly−X−Y repeating pattern. The geometric arrangement of the triple helix introduces three copies of the consensus sequence into one molecule and exposes the basic amino acids in the X and Y positions for interaction with HS or heparin, while the Gly residues are shielded from solvent (*28*).

HSPG binding by the collagen tail of AChE is one example of a biologically important ligand interaction involving triple-helical domains. Other examples include the binding of collagens to cell surface integrins, fibronectin, and matrix metalloproteinases, as well as heparin (*29*, *30*). In C1q and the mannose binding lectin, the triple-helix sites are critical for interactions with proteases and receptors, while the collagen triple-helical region is the ligand binding site of the macrophage scavenger receptor (*31*). Studies on the macrophage scavenger receptor and C1q suggest that triple-helical binding interactions largely involve charged residues, and although they show selectivity, they do not exhibit the same degree of specificity as seen for globular proteins (*32*−*35*). Several studies suggest that flexibility in the triple-helix domain is important for recognition. Examples include the presence of an imino acid poor region adjacent to the unique matrix metalloproteinase cleavage site in fibril forming collagens (*36*, *37*) and the location of destabilizing Gly−Gly−Y triplets flanking a type III collagen binding site for a monoclonal antibody (*38*, *39*). An understanding of the nature of the interaction between the collagen tail of AChE and heparin may clarify the features and requirements of recognition and specificity for ligand binding by triple-helix sites in collagen and other proteins.

A multiplicity of heparin binding strategies has been reported in proteins (*40*−*42*). Here, changes in conformation and thermal stability as a result of heparin binding are extended to peptide models of the collagen-like triple-helix domain in the asymmetric form of AChE. Triple-helical peptides were designed to model the two AChE heparin-binding sites, each containing one consensus sequence and the surrounding basic sequences. All peptides containing a consensus sequence have been shown to be capable of displacing asymmetric AChE from immobilized heparin and thus are good models for studying the interaction of heparin with the collagen tail of AChE (*43*). However, peptide models of the two binding sites differed in the degree of displacement of asymmetric AChE from heparin-coated plates, indicating nonequivalence of the two sites. To further clarify the nature of heparin binding, spectroscopic studies were performed on peptides modeling each of the heparin binding domains and homologous peptides containing substitutions for the basic residues, in the presence of varying concentrations of heparin, HS, and CS. Heparin led to an increased thermal stability for all peptides containing a consensus sequence. An increase in triple-helix content with increasing heparin concentration was seen for the two peptides that showed a high capacity to displace AChE from heparin, while the other peptides precipitated or showed no change. Similar effects were seen for HS but not for CS.

EXPERIMENTAL PROCEDURES

Peptide Synthesis and Purification. Peptides were synthesized by SynPep Corp. (Dublin, CA) using Fast-Moc method on *N*-(9-fluorenyl) methoxycarbonyl-RINK resin manually using solid-phase peptide synthesis procedures. The purity of the peptides was determined to be greater than 92% by reverse-phase analytical HPLC on a C-18 column using a linear gradient of CH_3CN (0.075% TFA) and H_2O (0.1% TFA) as the eluent. The identity of each peptide was confirmed using laser desorption mass spectrometry performed by the Protein and Carbohydrate Structure Facility at the University of Michigan (Ann Arbor, MI). Peptides were dried in vacuo over P_2O_5 for 48 h prior to weighing.

Circular Dichroism Spectroscopy (CD). CD spectra were recorded on an AVIV model 62DS spectropolarimeter equipped with a five-position thermostated cell holder controlled by a Hewlett-Packard Peltier temperature controller. Samples were transferred into quartz cells of path length 0.1 cm, which had been equilibrated at 0 °C, using pre-cooled pipet tips. Peptide solutions of approximately 1 mg/mL were used, with concentration determination by amino acid analysis (CSIRO, Australia). Peptide solutions (monomer concentration ∼350 μM) were dissolved in 0.15 M NaCl, 0.01M sodium phosphate, pH 7.4, and equilibrated for more than 48 h on ice and incubated overnight on ice with gentle mixing in the absence or presence of increasing amounts of heparin (Sigma) MW ∼ 6000 (10−800 μM). Similar studies were carried out with heparan sulfate (Sigma) MW ∼ 7500 (10−800 μM), polydisperse heparan sulfate (Sigma), and chondroitin sulfate (Sigma) MW ∼ 60 000 (1−80 μM). For chondroitin sulfate experiments, a concentration range 10-fold less than other GAGs was used since this GAG had a 10-fold higher molecular weight.

For wavelength scans, spectra were collected from 260 nm to approximately 200 nm with a step size of 0.5 nm and a bandwidth of 1.5 nm at 0 °C, corrected for buffer baseline and GAG contributions measured in the same cells. These results were normalized to mean residue ellipticities ([θ]). For thermal equilibrium melting, the wavelength at which measurements were recorded was kept constant at 225 nm, while the temperature was increased in increments of 0.3 °C followed by a 2-min equilibration at each temperature. Data were collected for 10 s at each temperature.

Calculation of Thermodynamic Parameters. The data obtained from the equilibrium melting for the peptides were fit to a two-state monomer to trimer transition model. The melting curves were normalized to the fraction of folded (F) or triple-helical peptide with

$$F = [\theta - \theta_m(T)]/[\theta_t(T) - \theta_m(T)] \quad (1)$$

where θ is the observed ellipticity of the sample and $\theta_t(T)$ and $\theta_m(T)$ are the ellipticities of the fully folded and fully unfolded states, respectively, with a correction for their

Table 1: Sequences of Peptides from *Torpedo* Collagen-Like Tail of AChE and Comparison of Their Biochemical and Biophysical Properties upon Addition of Heparin

Peptide	Peptide Sequence	$[\theta]_{225nm}$[a] -hep	$[\theta]_{225nm}$[b] +hep	$\Delta[\theta]_{225nm}$	T_m (°C)[c] -hep	T_m(°C) +hep[b]	ΔT_m
P146	NH_2-POG**R**OG**RKGR**OGV**R**GP**R**G$(POG)_4$-$CONH_2$[d]	1970	1970	0	15.5	24.6	+9.1
P251	NH_2-POG**R**OG**KRGK**TGL**K**GDIG$(POG)_4$-$CONH_2$	2000	2500	+500	9.8	15.8	+6.0
P146A	NH_2-POG**R**OG**AAGA**OGV**R**GP**R**G$(POG)_4$-$CONH_2$	2600	2500	-100	18.6	19.2	+0.6
P146B	NH_2-POG**A**OG**RKGR**OGV**A**GP**A**G$(POG)_4$-$CONH_2$	2000	2500	+500	11.0	17.9	+6.9
P251/P146	NH_2-POG**R**OG**KRGK**OGV**R**GP**R**G$(POG)_4$-$CONH_2$	2390	2285	-105	19.7	27.4	+7.7
$(POG)_{10}$	NH2-POGPOGPOGPOGPOGPOG$(POG)_4$-COOH	4700	4700	0	57.0	56.0	-1.0

[a] Units for mean residue ellipticity are deg cm^2 $dmol^{-1}$. [b] The mean residue ellipticity and thermal stability of peptides listed are for heparin (6000 MW) added at 800 μM. [c] Error for thermal transition temperatures is ±2%. [d] Consensus sequence residues are boxed. Basic residues are in bold; sites of basic residues surrounding consensus sequence are underlined.

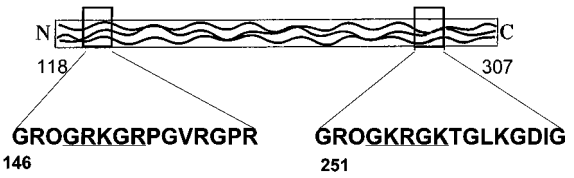

FIGURE 1: Schematic representation of the 189 residue triple-helical domain (residues 118−307) of the tail of asymmetric AChE. Within the collagen-like domain, two heparin binding domains are present. The approximate location and sequences incorporated into peptides are depicted with consensus sequences underlined.

temperature dependence by linear extrapolation of the pre- and post-transition regions of the thermal equilibrium curves. The equilibrium constant for the transitions, assuming a two-state mechanism in which a triple helix dissociates to three unfolded chains, is

$$K = [\text{trimer}]/[\text{monomer}] = c_n/c_u^3 = F/3c^2(1 - F)^3 \quad (2)$$

where $c_o = c_u + 3c_n$ is the total concentration of the peptide, c_n is the concentration of folded peptide, c_u is the concentration of unfolded peptide, and F is the fraction of the folded peptide as indicated above (*44*, *45*). The T_m was determined by curve fitting with the equation

$$\ln K(T) = (\Delta H°/RT)(T/T_m - 1) - \ln(0.75c^2) \quad (3)$$

following from $\Delta G° = \Delta H° - T\Delta S° = -RT\ln K$, where $\Delta G°$, $\Delta H°$, $\Delta S°$, R, T, and T_m are the standard free energy, enthalpy, entropy, gas constant, absolute temperature, and melting temperature, respectively. T_m was derived by fitting the normalized equilibrium melting curves to eq 3 using a nonlinear least-squares algorithm.

RESULTS

Peptide Design. The 30-mer peptides designed to model the N- and C-terminal heparin binding sites were designated as P146 and P251, respectively, according to their N-terminal residue in the *Torpedo* collagen-like tail sequence (ref *43*; Figure 1; Table 1). Peptide P146 contains the consensus sequence *GRKGR*, together with three flanking triplets, which are also rich in basic residues. Peptide P251 contains the consensus sequence *GKRGK*, also with flanking basic triplets. Four repeats of Pro−Hyp−Gly were added at the C-terminal end, and one Pro−Hyp−Gly triplet at the N-terminus, to promote the formation of a triple-helical structure and provide increased stability (*39*, *46*). Circular dichroism (CD) studies indicated that both P146 and P251 form stable triple helices and that P146 (T_m = 15.6 °C) is more thermally stable than P251 (T_m = 9.8 °C) (ref *43*; Table 1). All AChE model peptides have a lower mean residue ellipticity ($[\theta]_{225\ nm}$) and decreased thermal stability relative to the most rigid triple-helical 30-mer peptide, $(POG)_{10}$ (Table 1).

To examine the effect of basic residues within and surrounding the consensus sequence on interaction with heparin, peptides were designed, in which the three basic residues of the consensus sequence were replaced by alanine (P146A) or the three basic residues surrounding the consensus sequence were replaced by alanine (P146B). Previous CD studies demonstrated that peptide P146A has an increased thermal stability relative to wild-type P146 (T_m = 18.6 °C), while P146B demonstrated a stability lower than that of P146 (T_m = 11.0 °C) (ref *43*; Table 1). These peptides differed in their ability to displace whole enzyme asymmetric AChE from heparin-coated plates. At 5 μg/μL, the highest concentration examined, the displacement at 4 °C was 91% for P251, 65% for P146, and 92% for P146B. The triple-helical forms of peptides P146, P251, and P146B were far more efficient than the monomeric forms in displacement, while P146A displaced very little in both monomeric and trimeric forms (~15%) (*43*). $(POG)_{10}$ had only a negligible effect.

Effect of Heparin on the Conformation of AChE Collagen Tail Model Peptides. To examine the binding of heparin to peptides P146 and P251, each was incubated with increasing amounts of heparin ranging from 10 to 800 μM, corresponding to molar ratios ranging from approximately 1:12 to 6:1 heparin/triple-helical peptide. The CD spectra were monitored as a function of increasing concentrations of heparin to measure any peptide conformational change (Figure 2). The CD signal for heparin is of very low magnitude and was subtracted to isolate changes in peptide conformation. Incubation of P146 with heparin causes an initial decrease in the characteristic 225 nm maximum, with the lowest value occurring at an estimated heparin/triple-helical peptide molar ratio of 1:2 (Figure 2 and Figure 3, panel A). This decrease

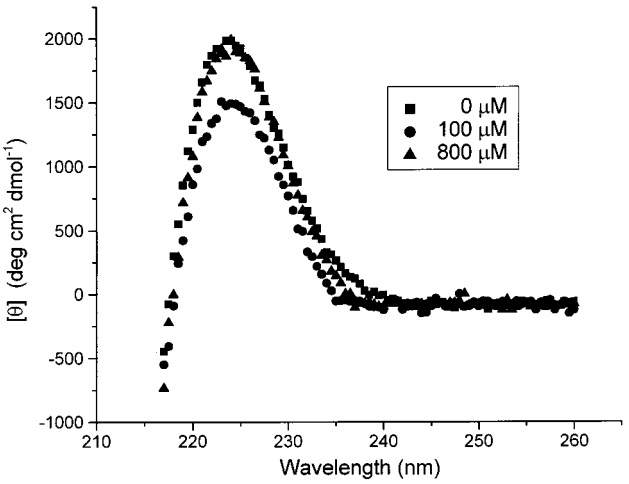

FIGURE 2: Circular dichroism spectra of peptide P146 in the presence and absence of heparin. Spectra were recorded in 0.01 M sodium phosphate, 0.15 M NaCl, pH 7.0, at 0 °C. The maximum near 225 nm is characteristic of the triple-helical conformation. The spectra are normalized to mean residue ellipticities ([θ]). Only two heparin concentrations are shown for clarity, although seven concentrations were used in the experiments. P146 with no heparin (■); P146 with 100 μM heparin (●); P146 with 800 μM (▲). The dynode voltages were monitored and were similar at 225 nm for samples that showed precipitation and those that did not. Slight variations in baseline between 250 and 260 nm as a result of turbidity were corrected and did not influence the trend observed for the change in ellipticity upon titration with increasing heparin concentration.

in ellipticity is concurrent with visual observation of a white precipitate. Upon further addition of heparin, P146 was resolubilized and regained most of the initial magnitude of $[\theta]_{225\ nm}$, suggesting that heparin had little effect on the triple-helical conformation of the peptide at high heparin/peptide ratios (Figure 2 and Figure 3, panel A). Similar studies on heparin incubation with P146A, in which the consensus sequence basic residues are replaced by alanine, demonstrated no significant change in $[\theta]_{225\ nm}$ for the entire concentration range of heparin studied (Figure 3, panel C; Table 1), but slight precipitation was observed at low heparin concentrations (Figure 3, panel C). For peptide P146B, in which surrounding basic residues are replaced by alanine, $[\theta]_{225\ nm}$ increased upon addition of heparin, exhibiting a maximum value at an approximate molar ratio of 1:1 heparin/triple-helical peptide (Figure 3, panel D; Table 1), and the value remained constant as more heparin was added. This pattern of $[\theta]_{225\ nm}$ increase is consistent with an enhancement of the triple-helical conformation in the peptide as low amounts of heparin are added, reaching a maximum value.

The peptide modeling the C-terminal heparin binding site, P251, demonstrated an increase in $[\theta]_{225\ nm}$ upon addition of heparin until it reached a plateau at a maximal value (Figure 3, panel B). Again, this suggests an increased content of triple helix upon binding of the peptide to heparin, reaching a final value. The maximum ellipticity at 225 nm is reached at an estimated molar ratio of 1:2 heparin/triple-helical peptide (Figure 3, panel B). No precipitation was observed. A control peptide $(POG)_{10}$ showed no significant increase in ellipticity and no precipitation upon incubation with increasing amounts of heparin (Table 1).

Effects of Thermal Stability of Model Peptides upon Incubation with Heparin. The thermal stability of each peptide was determined in the presence of 800 μM heparin, by monitoring the 225 nm maximum as a function of temperature. Equilibrium unfolding curves showed sharp cooperative transitions that can be fitted to a two-state trimer to monomer model. In the presence of heparin, increased thermal stabilities were demonstrated for P146, P146B, and P251, with the increase ranging from 6 °C (P251) to 9 °C (P146) (Figure 4; Table 1). Broadening of the thermal transitions was also observed in the presence of heparin and could result from heterogeneity in binding or could reflect a lower enthalpy of the transition when heparin is bound to the peptide. Addition of heparin did not affect the thermal stability of P146A, which does not contain the consensus sequence (Figure 4, panel C), or $(POG)_{10}$ (data not shown), indicating a requirement for the basic consensus sequence for interaction.

Peptides Modeling the Two Heparin Binding Domains Demonstrate Interaction with Other GAGS. Experiments identical to those described above were carried out with heparan sulfate, a GAG with the same disaccharide unit as heparin, but with decreased sulfation. Addition of heparan sulfate (MW ~ 7500) (1:12 to 6:1 HS/triple-helical peptide) to P146 and P251 resulted in changes in ellipticity and thermal stability similar to those observed for heparin (Figure 5, panels A and B; Table 2). When highly polydisperse heparan sulfate was employed in these experiments, a decrease in ellipticity and clouding of solution was observed for the peptides (data not shown).

Chondroitin sulfate, which has a different repeating disaccharide unit and a different conformation from heparan sulfate and heparin, was incubated with the AChE collagen-tail model peptides (1:100 to 1:4 heparin/triple-helical peptide) to determine the specificity of the interaction of peptides among different GAGs. Chondroitin sulfate did affect the ellipticity of all peptides but in a manner distinct from that observed for heparin and heparan sulfate. In particular, a decrease in the 225 nm band was observed, together with a clouding of the solution in all cases (Figure 5, panels A and B; Table 2). The cloudiness contrasts with the solid white precipitate seen for P146 and P146A after heparin addition. Small increases in thermal stability were demonstrated for all peptides in the presence of chondroitin sulfate, varying from 4 °C (P251) to 7 °C (P146) (Table 2). These results suggest that the polyanionic chondroitin sulfate is interacting with the basic model peptides, leading to a small degree of stabilization but that its mode of interaction is distinct from that of heparin and heparan sulfate.

Interaction of a Chimeric Peptide with GAGs. A chimeric peptide P251/P146 was designed in which the consensus sequence of peptide P251 (GKRGK) has the surrounding sequence of peptide P146 (Table 1). Peptide P251/P146 was shown to be triple helical, with a $[\theta]_{225\ nm}$ of 2390 deg cm^2 dmol^{-1} and a thermal stability of 19.7 °C (Table 1), a T_m higher than both P251 and P146. P251/P146 showed behavior similar to P251 in the presence of heparin and heparan sulfate but demonstrated a loss of ellipticity similar to P146 in the presence of chondroitin sulfate (Figure 5, panel C). The thermal stability of P251/P146 was increased approximately 5 °C in the presence of a high concentration of CS and approximately 8 °C in the presence of heparin or HS (Table 2).

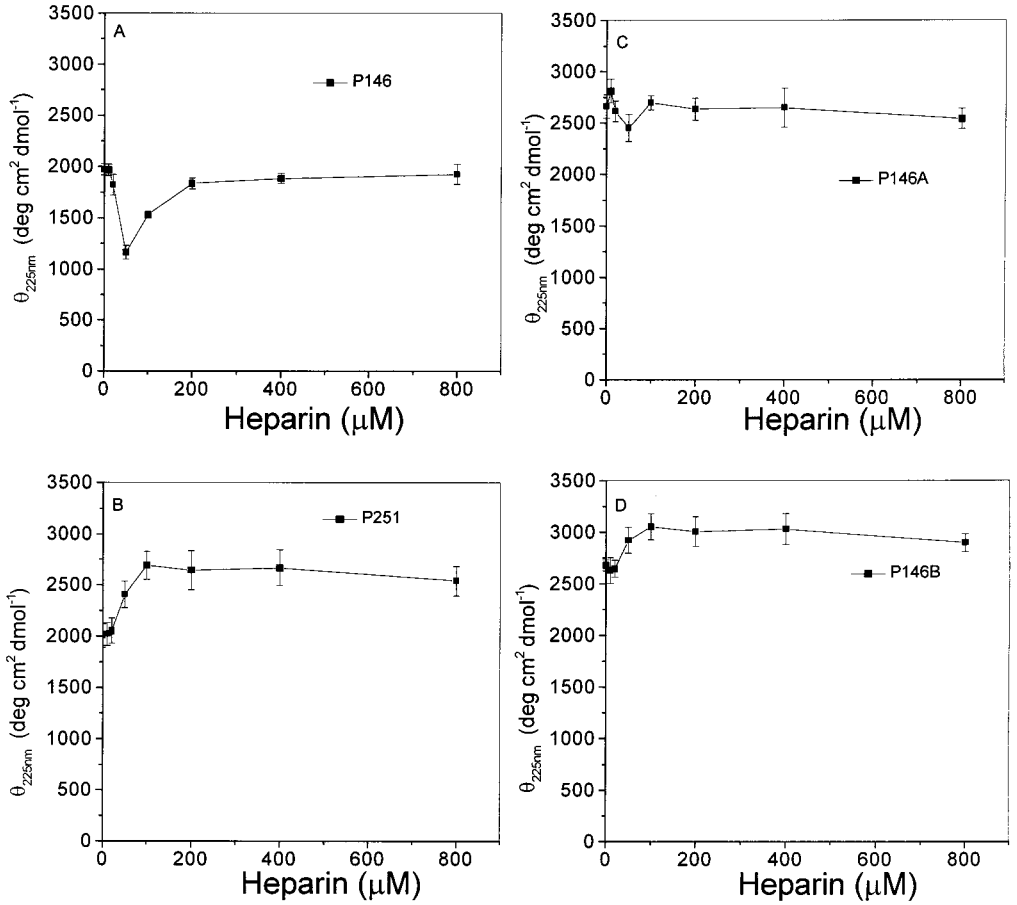

FIGURE 3: Change in the mean residue ellipticities at 225 nm ($[\theta]_{225\ nm}$) for triple-helical AChE peptide models upon incubation with increasing concentrations of heparin from 0 to 800 μM. (A) P146; (B) P251; (C) P146A; (D) P146B. Fitting hyperbolic plots for P146B and P251 for one-site binding suggests an estimated binding constant between 10 and 50 μM heparin concentration, assuming an approximate homogeneous preparation of 6000 MW heparin.

DISCUSSION

Physiological properties of GAGs are largely mediated by their interaction with proteins. Heparin binds to antithrombin III to inhibit blood coagulation (*47*), while heparan sulfate in HSPG binds to extracellular matrix components (ECM) and is involved in the localization of proteins, such as asymmetric AChE, to their site of action (*9*, *12*, *48*, *49*). Protein sites that bind to heparin and HS consist of basic residues included in α-helices, β-sheets, loops, or more complex three-dimensional conformations (*50*−*57*). In several proteins and in model peptides, heparin binding has been observed to change the α-helical or β-sheet content and/or to increase stability (*58*−*63*). The studies reported here extend the understanding of GAG interactions to the collagen triple helix in asymmetric AChE.

The recent work of Verrecchio et al. (*63*) emphasizes the necessity for multiple copies of a consensus sequence in close proximity for enhanced heparin binding. The triple-helix structure innately provides such multiple consensus sequences. Consistent with this concept is the observation that monomer peptide models of AChE heparin binding sites have a much weaker displacement of asymmetric AChE from heparin-coated plates than trimers (*43*). The high axial rise and rather small radius of the triple helix result in a very high density of positive charge from the basic residues of the three heparin-binding consensus sequences (*64*). Recently, modeling studies suggest that charge distribution and concentration in a triple helix are likely to promote the binding of more than one polyanionic heparin molecule through electrostatic interactions (*28*). The two triple-helical heparin binding domains within the AChE collagen tail differ in their ability to displace AChE from immobilized heparin and allow an analysis of the specificity and nature of the heparin interaction with the collagen triple-helix motif.

The stable triple-helical peptide models of the two AChE collagen tail binding sites were observed to show distinctive binding properties dependent on both the consensus sequence and the tripeptide sequences surrounding the consensus sequence. In this peptide set, peptides P251, modeling the C-terminal heparin binding site, and P146B, in which the basic residues surrounding the N-terminal consensus sequence were replaced by alanine residues, were found to have the lowest thermal stability and the highest displacement capacity, suggesting a stronger interaction with heparin. A role for local triple-helix instability in the binding of heparin has been suggested (*43*). The studies reported here show that these two peptides, P251 and P146B, both exhibit an increase in triple-helix content as increasing amounts of heparin were added, reaching a maximum value. Heparin binding to the more flexible, less stable basic regions of these peptides could reduce charge repulsion and lead to the higher triple-helix content demonstrated by the increase in $[\theta]_{225\ nm}$. The observed increase in triple-helix content could be caused by a reinforcement of the triple-helix parameters when there is

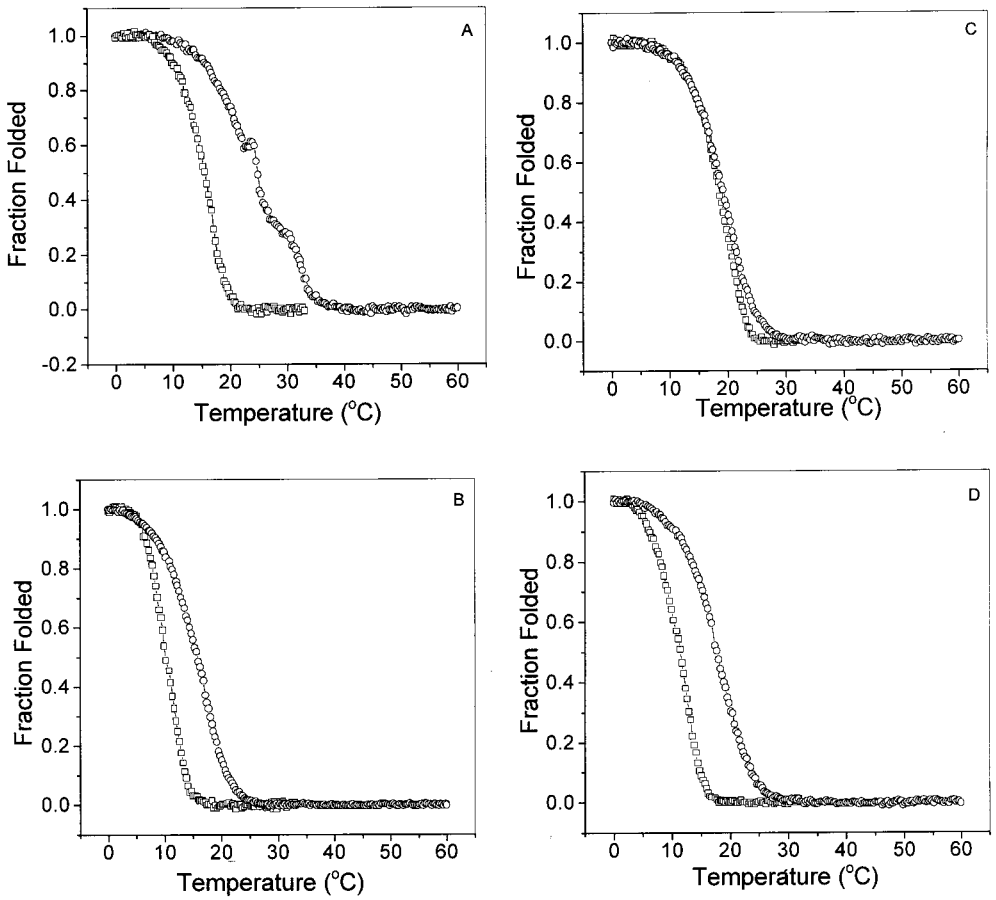

FIGURE 4: Thermal stability of AChE model peptides in the absence (□) and presence (○) of 800 μM heparin for (A) P146; (B) P251; (C) P146A; (D) P146B. Equilibrium thermal melting profiles monitored at 225 nm were normalized to fraction folded for peptides. In the presence of heparin, an increased stability is observed for all peptides that contain a consensus sequence. P146A, in which the basic residues of the consensus sequence are substituted by alanine, does not undergo a significant increase in melting temperature. Note the apparent multiple transitions for P146 in the presence of heparin. A measure of the dynode voltage during the thermal melt of this sample demonstrated a temperature-dependent aggregation of the peptide and/or peptide−heparin complex, followed by a resolubilization at higher temperatures.

a parallel, in register, binding of heparin to the triple helix (Figure 6, panel A). Such reinforcement could occur along a substantial distance, since the length of heparin molecules in the 6000 MW preparation used is similar to that of the triple-helical peptides studied (Figure 6). Heparin helical molecules bound parallel and in register to collagen triple helices could provide repetitive electrostatic interactions because of the close match between the axial supercoil repeat of the collagen helix (~8.7 Å) and the axial translation of the repeating disaccharide unit of heparin (~8.0−8.7 Å) (Figure 6, panel A; ref *28*). This reinforcement, including the possibility of one heparin molecule binding to at least two chains of the triple helix, could promote an increased triple-helix content or a more rigid triple-helix conformation (Figure 6, panel B). This mode of binding is reminiscent of the increased α-helix content seen for the addition of heparin to model heparin binding peptides (*59*, *63*) and papain (*62*).

In contrast, peptide P146, which models the N-terminal binding site, shows initial precipitation at low heparin/peptide ratios, followed by resolubilization and no significant effect on triple-helix content. This mode of binding is reminiscent of the aggregation observed in the binding of cardiotoxin and heparin at high cardiotoxin/GAG ratios (*65*). At low heparin concentrations, more than one peptide must bind one heparin molecule, leading to the formation of a complex and aggregation for the P146−heparin interaction. With increasing GAG concentration, more heparin becomes available to interact with each peptide. This could lead to resolubilization. Replacement of the consensus sequence basic residues of P146 with Ala residues (P146A) showed less precipitation and no significant change in the triple-helix content. As compared with P251 and P146B, peptides P146 and P146A have a higher stability and may have less flexibility in the consensus region. Both P146 and P146A peptides have a distribution of three basic charges surrounding the consensus sequence of the N-terminal site. A staggered mode of interaction for P146 is possible as a result of flanking charged residues (Figure 6, panel C). This staggered mode of interaction may not allow a reinforcement of triple-helical content of the peptide but may promote precipitation since one heparin molecule has the ability to bind more than one peptide (Figure 6, panel C). The chimeric model peptide, with the consensus sequence of P251 and the surrounding residues of P146, showed heparin and HS binding similar to that of P251 but CS interaction similar to that of P146. Subtle changes in the triple-helix interaction with GAGs appear to relate to the nature and distribution of the basic residues and surrounding sequences in this uniform triple-helical conformation. Previous studies have indicated that arginine was more effective than lysine in binding GAGs (*66*), but it is interesting to note that the most arginine-rich peptide, P146 (5 Arg, 1 Lys), has a lower displacement ability

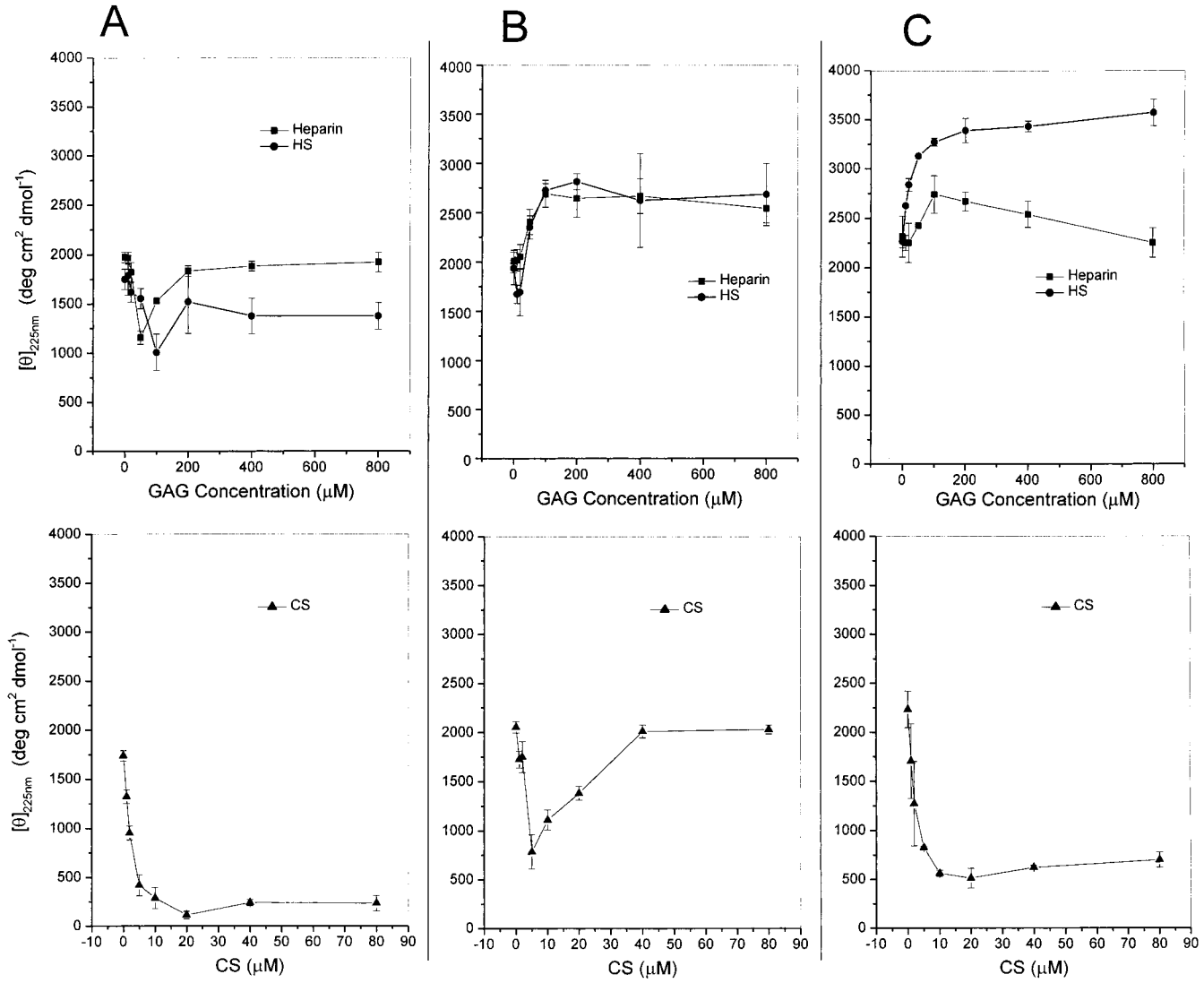

FIGURE 5: Change in the mean residue ellipticities at 225 nm ($[\theta]_{225\ nm}$) for triple-helical AChE peptide models (A) P146, (B) P251, and (C) P251/P146 upon incubation with increasing concentrations of heparin (■) and heparan sulfate (●) from 0 to 800 μM (top panels A−C) and chondroitin sulfate (▲) from 0 to 80 μM (bottom panels A−C).

Table 2: Binding of Peptides from *Torpedo* Collagen-Like Tail of AChE to Heparan Sulfate and Chondroitin Sulfate

		Heparin[a]		Heparan Sulfate[b]		Chondroitin Sulfate[c]	
Peptide	**Peptide Sequence**	**$\Delta[\theta]_{225nm}$**	**ΔT_m[d]**	**$\Delta[\theta]_{225nm}$**	**ΔT_m**	**$\Delta[\theta]_{225nm}$**	**ΔT_m**
P146	NH_2-POG**R**OG[RKGR]OGV**R**GP**R**G$(POG)_4$-$CONH_2$[e]	0	+9.1	-1200	+10.5	-1500	+7.0
P251	NH_2-POG**R**OG[KRGK]TGL**K**GDIG$(POG)_4$-$CONH_2$	+500	+6.0	+500	+5.4	-50	+4.0
P251/P146	NH_2-POG**R**OG[KRGK]OGV**R**GP**R**G$(POG)_4$-$CONH_2$	-105	+7.7	-105	+7.7	-1500	+5.8

[a] $\Delta[\theta]_{225\ nm}$ and ΔT_m upon addition of 800 μM heparin (MW∼ 6000). [b] $\Delta[\theta]_{225\ nm}$ and ΔT_m upon addition of 800 μM heparan sulfate (MW∼ 7500). [c] $\Delta[\theta]_{225\ nm}$ and ΔT_m upon addition of 80 μM chondroitin sulfate (MW∼ 60000). Units for mean residue ellipticity and T_m are deg cm^2 dmol^{-1} and °C, respectively. [d] Error for thermal transition temperatures is ±2%. [e] Consensus sequence residues are boxed. Basic residues are in bold; sites of basic residues surrounding consensus sequence are underlined.

than the more lysine-rich P251 (2 Arg, 3 Lys).

Increased thermal stability was observed for all peptides in the presence of a high concentration of heparin, except for $(POG)_{10}$ and P146A, which lacked the consensus sequence. This increase in thermal stability is expected for binding between peptides and heparin and is similar to the increased thermal stability reported for heparin binding by α-helical model peptides, acidic FGF, and basic FGF (*59*, *60*, *67*, *68*). The amount of increase in the melting temperature does not show any correlation with the original thermal stability of the collagen-like peptides or the modes of binding.

The addition of heparan sulfate, which resembles heparin in its disaccharide repeating unit, but differs in sulfation, showed similar conformational and stabilizing effects on the AChE model peptides, while addition of chondroitin sulfate resulted in a loss of ellipticity, cloudiness, and a smaller

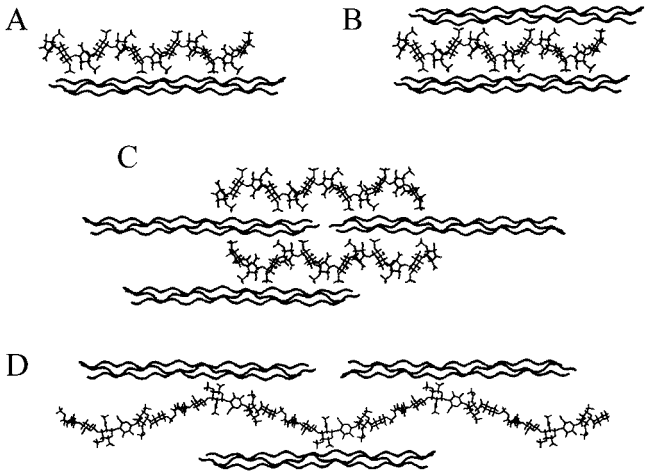

FIGURE 6: Schematic diagram of proposed modes of GAG binding to triple-helical peptide models. (A) In register, parallel interaction of one triple-helical peptide with one heparin molecule. (B) Proposed interaction for an in register interaction of one heparin molecule with two triple-helical peptides. (C) Proposed staggered interaction of triple-helical peptides with heparin involving charged residues surrounding the consensus site. This could result in the formation of a network and resultant precipitation. (D) Proposed interaction of triple-helical peptide with CS. The helical repeat of CS is much longer than that of the triple helix so that interactions can occur only locally at distant intervals, making the interaction less specific and probably weaker. A long CS chain could accommodate several peptide molecules, creating a clouding of the sample without precipitation (*28*).

increase in thermal stability. Clearly, chondroitin sulfate is interacting with the peptides but in a very different way from that seen for heparin and HS. This possibility is consistent with the capacity of HS to displace AChE from tissue and heparin-coated plates, while CS could not (*8*, *9*, *43*). The CS interaction with peptides (Figure 6, panel D) appears to correlate with the number of basic residues present in each peptide, suggesting a nonspecific interaction. The cloudiness observed for the interaction with CS in these particular cases may be the result of the interaction of a long CS chain with several peptides (Figure 6, panel D). The fact that a precipitate is not seen could be due to a low affinity of binding.

The studies on heparin binding by the AChE collagen tail model peptides present an opportunity for clarifying the nature of binding of ligands to collagen triple-helix domains. Clusters of basic residues have been implicated in the binding of ligands by the collagen-like domain of the homotrimeric macrophage scavenger receptor (*32*, *70*−*71*), while a highly charged region with both basic and acidic residues has been proposed as a binding domain in the collagen tail of C1q (*34*, *35*). The mode of collagen binding is not known, although results suggest a broad but discriminating recognition by triple-helical domains (*69*). The results on heparin binding by the AChE tail collagen-like model peptides suggest that the inherent presence of multiple binding sequences in a homotrimeric collagen triple helix may enhance binding. Such 3-fold screw symmetry, together with spacing of basic residues in the X and Y positions, may provide the potential for alternate modes of binding with other linear biomolecules, such as GAGs. The strength and nature of the heparin−peptide interactions also appear to support a role for sequence-modulated flexibility of the collagen triple helix in GAG binding, a feature observed for other triple-helical−ligand interactions (*36*, *37*, *39*).

ACKNOWLEDGMENT

We thank Dr. John Ramshaw and Mr. Nick Bartone for amino acid analysis. We are also grateful to Drs. John Ranshaw, Konrad Beck, Daniel Pilch, and Marilyn Sanders for helpful discussions.

REFERENCES

1. Hall, Z. W., and Kelly, R. B. (1971) *Nat. New. Biol. 232*, 62−63.
2. Taylor, P., and Radic, Z. (1994) *Annu. Rev. Pharmacol. Toxicol. 34*, 281−320.
3. McMahan, U. J., Sanes, J. R., and Marshall, L. M. (1978) *Nature 271*, 172−4.
4. Bon, S., Vigny, M., and Massoulie, J. (1979) *Proc. Natl. Acad. Sci. U.S.A. 76*, 2546- 50.
5. Inestrosa, N. C., Silberstein, L., and Hall, Z. W. (1982) *Cell 29*, 71−9.
6. Vigny, M., Martin, G. R., and Grotendorst, G. R. (1983) *J. Biol. Chem. 258*, 8794−8798.
7. Brandan, E., and Inestrosa, N. C. (1984) *Biochem. J. 221*, 415−22.
8. Brandan, E., Maldonado, M., Garrido, J., and Inestrosa, N. C. (1985) *J. Cell. Biol. 101*, 985−92.
9. Casanueva, O. I., Garcia-Huidobro, T., Campos, E. O., Aldunate, R., Garrido, J., and Inestrosa, N. C. (1998) *J. Biol. Chem. 273*, 4258−65.
10. Deprez, P. N., and Inestrosa, N. C. (1995) *J. Biol. Chem. 270*, 11043−6.
11. Cardin, A. D., and Weintraub, H. J. (1989) *Arteriosclerosis 9*, 21−32.
12. Jackson, R. L., Busch, S. J., and Cardin, A. D. (1991) *Physiol. Rev. 71*, 481−539.
13. Tsilibary, E. C., Koliakos, G. G., Charonis, A. S., Vogel, A. M., Reger, L. A., and Furcht, L. T. (1988) *J. Biol. Chem. 263*, 19112−8.
14. Koliakos, G. G., Kouzi-Koliakos, K., Furcht, L. T., Reger, L. A., and Tsilibary, E. C. (1989) *J. Biol. Chem. 264*, 2313−23.
15. Yaoi, Y., Hashimoto, K., Koitabashi, H., Takahara, K., Ito, M., and Kato, I. (1990) *Biochim. Biophys. Acta 103*, 139−145.
16. Miles, A. J., Skubitz, A. P., Furcht, L. T., and Fields, G. B. (1994) *J. Biol. Chem. 269*, 30939−45.
17. San Antonio, J. D., Lander, A. D., Karnovsky, M. J., and Slayter, H. S. (1994) *J. Cell Biol. 125*, 1179−88.
18. Delacoux, F., Fichard, A., Cogne, S., Garrone, R., and Ruggiero, F. (2000) *J. Biol. Chem. 275*, 29377−82.
19. Sweeney, S. M., Guy, C. A., Fields, G. B., and San Antonio, J. D. (1998) *Proc. Natl. Acad. Sci. U.S.A. 95*, 7275−80.
20. Rich, A., and Crick, F. H. C. (1961) *J. Mol. Biol. 3*, 483−506.
21. Ramachandran, G. N. (1967) Structure of Collagen at the Molecular Level, in *Treatise on Collagen* (Ramachandran, G. N., Ed.) Vol. 1, pp 103−183, Academic Press, New York.
22. Fraser, R. D. B., MacRae, T. P., and Suzuki, E. (1979) *J. Mol. Biol. 129*, 463−481.
23. Bella, J., Eaton, M., Brodsky, B., and Berman, H. (1994) *Science 266*, 75−81.
24. Jones, E. Y., and Miller, A. (1991) *J. Mol. Biol. 218*, 209−19.
25. Berg, R. A., and Prockop, D. J. (1973) *Biochemistry 12*, 3395−401.
26. Sakakibara, S., Inouye, K., Shudo, K., Kishida, Y., Kobayashi, Y., and Prockop, D. J. (1973) *Biochim. Biophys. Acta 303*, 198−202.
27. Heidemann, E., and Roth, W. (1982) *Adv. Polym. Sci. 43*, 143−203.
28. Deprez, P. N., and Inestrosa, N. C. (2000) *Protein Eng. 13*, 27−34.

29. Kadler, K. (1994) Type I Collagen (Collagen I), in *Extracellular Matrix I: Fibril Forming Collagens* (Sheterline, P., Ed.) Vol. 1, pp 550−560, Academic Press, London.
30. San Antonio, J. D., Slover, J., Lawler, J., Karnovsky, M. J., and Lander, A. D. (1993) *Biochemistry 32*, 4746−55.
31. Brodsky, B., and Shah, N. K. (1995) *FASEB J. 9*, 1537−46.
32. Doi, T., Higashino, K., Kurihara, Y., Wada, Y., Miyazaki, T., Nakamura, H., Uesugi, S., Imanishi, T., Kawabe, Y., Itakura, H., et al. (1993) *J. Biol. Chem. 268*, 2126−33.
33. Acton, S., Resnick, D., Freeman, M., Ekkel, Y., Ashkenas, J., and Krieger, M. (1993). *J. Biol. Chem. 268*, 3530−7.
34. Bradley, A. J., Brooks, D. E., Norris-Jones, R., and Devine, D. V. (1999) *Biochim. Biophys. Acta 1418*, 19−30.
35. Bradley, A. J., Maurer-Spurej, E., Brooks, D. E., and Devine, D. V. (1999) *Biochemistry 38*, 8112−23.
36. Fields, G. B. (1991) *J. Theor. Biol. 153*, 585−602.
37. Fan, P., Li, M. H., Brodsky, B., and Baum, J. (1993) *Biochemistry 32*, 13299−309.
38. Glattauer, V., Werkmeister, J. A., Kirkpatrick, A., and Ramshaw, J. A. (1997) *Biochem. J. 323*, 45−9.
39. Shah, N. K., Sharma, M., Kirkpatrick, A., Ramshaw, J. A., and Brodsky, B. (1997) *Biochemistry 36*, 5878−83.
40. Rosenberg, R. D., and Damus, P. S. (1973) *J. Biol. Chem. 248*, 6490−505.
41. Yamada, K. M., Kennedy, D. W., Kimata, K., and Pratt, R. M. (1980) *J. Biol. Chem. 255*, 6055−63.
42. Yabkowitz, R., Lowe, J. B., and Dixit, V. M. (1989) *J. Biol. Chem. 264*, 10888−96.
43. Deprez, P., Doss-Pepe, E., Brodsky, B., and Inestrosa, N. C. (2000) *Biochem. J. 350*, 283−290.
44. Engel, J., Chen, H. T., Prockop, D. J., and Klump, H. (1977) *Biopolymers 16*, 601−622.
45. Marky, L. A., and Breslauer, K. J. (1987) *Biopolymers 26*, 1601−20.
46. Yang, W., Chan, V. C., Kirkpatrick, A., Ramshaw, J. A., and Brodsky, B. (1997) *J. Biol. Chem. 272*, 28837−40.
47. Thunberg, L., Backstrom, G., and Lindahl, U. (1982) *Carbohydr. Res. 100*, 393−410.
48. Ruoslahti, E. (1988) *Annu. Rev. Cell Biol. 4*, 229−55.
49. San Antonio, J. D., Slover, J., Lawler, J., Karnovsky, M. J., and Lander, A. D. (1993) *Biochemistry 32*, 4746−55.
50. Calaycay, J., Pande, H., Lee, T., Borsi, L., Siri, A., Shively, J. E., and Zardi, L. *J. Biol. Chem. 260*, 12136−41.
51. Fretto, L. J., Fowler, W. E., McCaslin, D. R., Erickson, H. P., and McKee, P. A. (1986). *J. Biol. Chem. 261*, 15679−89.
52. Zhu, X., Komiya, H., Chirino, A., Faham, S., Fox, G. M., Arakawa, T., Hsu, B. T., and Rees, D. C. (1991) *Science 251*, 90−3.
53. Boissinot, M., Kuhn, L. A., Lee, P., Fisher, C. L., Wang, Y., Hallewell, R. A., and Tainer, J. A. (1993) *Biochem. Biophys. Res. Commun. 190*, 250−6.
54. Moy, F. J., Seddon, A. P., Campbell, E. B., Bohlen, P., and Powers, R. (1995) *J. Biomol. NMR 6*, 245−54.
55. Moy, F. J., Seddon, A. P., Bohlen, P., and Powers, R. (1996) *Biochemistry 35*, 13552−61.
56. Elisen, M. G., Maseland, M. H., Church, F. C., Bouma, B. N., and Meijers, J. C. (1996) *Thromb. Haemost. 75*, 760−6.
57. Jin, L., Abrahams, J. P., Skinner, R., Petitou, M., Pike, R. N., and Carrell, R. W. (1997) *Proc. Natl. Acad. Sci. U.S.A. 94*, 14683−8.
58. Cardin, A. D., Demeter, D. A., Weintraub, H. J., and Jackson, R. L. (1991) *Methods Enzymol. 203*, 556−83.
59. Ferran, D. S., Sobel, M., and Harris, R. B. (1992) *Biochemistry 31*, 5010−6.
60. Prestrelski, S. J., Fox, G. M., and Arakawa, T. (1992) *Arch. Biochem. Biophys. 293*, 314−9.
61. Skinner, R., Abrahams, J. P., Whisstock, J. C., Lesk, A. M., Carrell, R. W., and Wardell, M. R. (1997) *J. Mol. Biol. 266*, 601−9.
62. Almeida, P. C., Nantes, I. L., Rizzi, C. C., Judice, W. A., Chagas, J. R., Juliano, L., Nader, H. B., and Tersariol, I. L. (1999) *J. Biol. Chem. 274*, 30433−8.
63. Verrecchio, A., Germann, M. W., Schick, B. P., Kung, B., Twardowski, T., and San Antonio, J. D. (2000) *J. Biol. Chem. 275*, 7701−7707.
64. Beck, K., and Brodsky, B. (1998) *J. Struct. Biol. 122*, 17−29.
65. Patel, H. V., Vyas, A. A., Vyas, K. A., Liu, Y. S., Chiang, C. M., Chi, L. M., and Wu, W. G. (1997) *J. Biol. Chem. 272*, 1484−92.
66. Fromm, J. R., Hileman, R. E., Caldwell, E. E., Weiler, J. M., and Linhardt, R. J. (1995) *Arch. Biochem. Biophys. 323*, 279−87.
67. Tsai, P. K., Volkin, D. B., Dabora, J. M., Thompson, K. C., Bruner, M. W., Gress, J. O., Matuszewska, B., Keogan, M., Bondi, J. V., and Middaugh, C. R. (1993) *Pharm. Res. 10*, 649−59.
68. Volkin, D. B., Tsai, P. K., Dabora, J. M., Gress, J. O., Burke, C. J., Linhardt, R. J., and Middaugh, C. R. (1993) *Arch. Biochem. Biophys. 300*, 30−41.
69. Krieger, M., Acton, S., Ashkenas, J., Pearson, A., Penman, M., and Resnick, D. (1993) *J. Biol. Chem. 268*, 4569−72.
70. Tanaka, T., Nishikawa, A., Tanaka, Y., Nakamura, H., Kodama, T., Imanishi, T., and Doi, T. (1996) *Protein Eng. 9*, 307−13.
71. Yamamoto, K., Nishimura, N., Doi, T., Imanishi, T., Kodama, T., Suzuki, K., and Tanaka, T. (1997) *FEBS Lett. 414*, 182−6.

BI001108U